ISSN 1067-8212, Russian Journal of Non-Ferrous Metals, 2017, Vol. 58, No. 1, pp. 30–35. © Allerton Press, Inc., 2017.
Original Russian Text © A.N. Efremov, V.A. Khokhlov, S.V. Isupov, Yu.P. Zaykov, 2016, published in Izvestiya Vysshikh Uchebnykh Zavedenii, Tsvetnaya Metallurgiya, 2016, No. 6, pp. 14–20.

## METALLURGY OF NONFERROUS METALS

# Modeling of Electric and Thermal Fields in an Electrolyzer with Liquid-Metal Electrodes

**A. N. Efremov[a, *], V. A. Khokhlov[a, b, **], S. V. Isupov[a, ***], and Yu. P. Zaykov[a, b, ****]**

[a] *Institute of High-Temperature Electrochemistry, Ural Branch, Russian Academy of Sciences, Yekaterinburg, 620219 Russia*

[b] *Ural Federal University, Yekaterinburg, 620002 Russia*

**e-mail: alexandr_efremoff@mail.ru*

***e-mail: vladkhokh@mail.ru*

****e-mail: isupov.s.v@mail.ru*

*****e-mail: dir@ihte.uran.ru*

Received May 18, 2015; accepted for publication in final form, June 30, 2015

**Abstract**—The influence of the molten electrolyte composition and geometric configuration of the electrolyzer with liquid-metal lead electrodes on the spatial distribution of dc and temperature in an apparatus of the "crucible-in-crucible" type, which is considered a prototype of the device to process spent nuclear fuel, is studied by mathematical modeling. It is shown that the calculated model parameters are in good agreement with the experimental data.

*Keywords:* modeling, electric field, thermal field, refining, liquid-metal electrodes

**DOI:** 10.3103/S1067821217010047

## INTRODUCTION

A promising pyroelectrochemical regeneration technology of nuclear fuel after its extraction from the reactor, which is performed in electrolyzers with molten salt electrodes and liquid-metal electrodes, is considered to solve the problems on the development of a closed fuel cycle for the innovative fast neutron nuclear reactors [1–6]. Heat-resistant and radiation-stable halogenide melts are recommended as electrolytes, while such metals as zinc, cadmium, lead, bismuth, tin, gallium, and their alloy can be used to fabricate electrodes [5–8]. These metals have relatively low melting points and will be in a liquid state under the salt melt layer during the electrolysis. Herewith, actinides (uranium, plutonium, etc.) are dissolved on the anode and deposited on the cathode; other impurities remain in the anodic alloy.

If the modes of the electrolytic process are selected correctly and thermodynamics of formation of metal alloys (which are deposited on the cathode) with the electrode material is known, high separation factors of metals with close electrode potentials, for example, actinides and lanthanides, can be attained. It is known from scientific and technical publications that constructions of the crucible-in-crucible type are preferentially considered for electrochemical processing of such materials [9–12]. However, even when using liquid-metal electrodes, it is impossible to exclude the nonuniform current distribution over their surface similarly to the case with solid metallic electrodes.

The authors of [13] showed that the actual (experimentally measured) current density on various segments of a lead anode could differ from the average one calculated over its total surface area more than twofold. This circumstance affects the heat and mass transfer both in molten salt electrodes and in liquid-metal electrodes. The nonuniform current distribution over the surface of liquid-metal electrodes should be also taken into account when selecting optimal process parameters of the electrolytic process, as well as when developing new designs of electrolyzers in order to attain high separation factors of metals with similar properties.

The experimental investigation into the processes of heat, mass, and charge transfer in above-described facilities is not a simple problem, especially when operating with aggressive molten salts and radioactive substances. This circumstance complicates detailed investigation and determination of parameters of these processes for the search for optimal electrochemical modes, since it requires numerous laborious experiments, which substantially prolongs the time of the development and creation of new technologies [14]. Apparent advantages when selecting optimal process parameters of a multifactor electrolytic process are inherent to the methods of mathematical modeling of electrical and thermal fields with the help of applied

software packages with the subsequent experimental verification of the performed calculations.

In this article we present the results of mathematical modeling of electrical and thermal fields as the functions of the electrolyte composition and geometry of the electrochemical cell of the crucible-in-crucible type with the KCl–$PbCl_2$ melt and lead electrodes, which is considered a prototype of the facility for pyroelectrochemical processing of anthropogenic feedstock. The results of modeling are compared with the experimental data [13].

## EXPERIMENTAL

### *Main Equations of Electrical and Thermal Conductivity*

To create a mathematical model describing the electrical and thermal fields in an electrolyzer with liquid-metal electrodes, we used the differential equations of electrical and thermal conductivity [14–16].

**Electric field.** The electric field in the conducting medium under the dc current passage is described according to the first Kirchhoff law and Ohm law with the help of the following equation [15]:

$$\operatorname{div}(\lambda\nabla\varphi) = 0, \tag{1}$$

where φ is the potential, V, and λ is the symmetric electrical conductivity tensor, which can be written for the isotropic conductor in the form

$$\lambda = \begin{pmatrix} \lambda & 0 & 0 \\ 0 & \lambda & 0 \\ 0 & 0 & \lambda \end{pmatrix}, \tag{2}$$

where $\lambda = f(T)$ is the temperature-dependent electrical conductivity, $\Omega^{-1}\ m^{-1}$.

For the isotropic nonuniform conductor or conductor with a variable temperature field $T(x, y, z) \neq$ const, Eq. (1) takes the following form:

$$\frac{\partial}{\partial x}\left(\lambda\frac{\partial\varphi}{\partial x}\right) + \frac{\partial}{\partial y}\left(\lambda\frac{\partial\varphi}{\partial y}\right) + \frac{\partial}{\partial z}\left(\lambda\frac{\partial\varphi}{\partial z}\right) = 0. \tag{3}$$

To find the unambiguous solution of Eq. (3), we specified the following boundary conditions:

(i) potential $\varphi = 0$ is specified on the outer end surface of the cathodic current led;

(ii) current $I = 23.2$ A is specified in the outer surface of the anodic current led allowing for the geometric cell sizes;

(iii) there is no current along the normal to the surface on the boundary with dielectric:

$$\lambda_x\frac{\partial\varphi}{\partial x}l_x + \lambda_y\frac{\partial\varphi}{\partial y}l_y + \lambda_z\frac{\partial\varphi}{\partial z}l_z = 0. \tag{4}$$

**Temperature field.** The thermal conductivity equation for the time-dependent problem has the form [16]

$$\operatorname{div}(k\nabla T) + Q = \rho c\frac{\partial T}{\partial t}, \tag{5}$$

or

$$\begin{aligned}&\frac{\partial}{\partial x}\left(k_x\frac{\partial T}{\partial x}\right) + \frac{\partial}{\partial y}\left(k_y\frac{\partial T}{\partial y}\right)\\ &+ \frac{\partial}{\partial z}\left(k_z\frac{\partial T}{\partial z}\right) + Q = \rho c\frac{\partial T}{\partial t},\end{aligned} \tag{6}$$

where $T$ is the temperature, K; $k_x$, $k_y$, and $k_z$ are temperature-dependent thermal conductivity coefficients in the direction of axes $X$, $Y$, and $Z$, W/(m K); ρ is the material density, $kg/m^3$; $c$ is the specific heat capacity, J/(kg K); $t$ is time, s; and $Q$ is heat, $W/m^3$, which is released during the electric current passage and is expressed as follows:

$$\begin{aligned}Q &= \lambda_x H_x^2 + \lambda_y H_y^2 + \lambda_z H_z^2\\ &= \lambda_x\left(\frac{\partial\varphi}{\partial x}\right)^2 + \lambda_y\left(\frac{\partial\varphi}{\partial y}\right)^2 + \lambda_z\left(\frac{\partial\varphi}{\partial z}\right)^2.\end{aligned} \tag{7}$$

When determining the temperature field in a laboratory cell, the stationary problem was solved; therefore, the right side of Eqs. (5)–(6) equals zero. To evaluate the stationary temperature field according to formula (6), boundary conditions should be specified:

(i) the temperature on the surface of the anodic cup corresponds to the temperature of the calculation variant

$$T = f(x, y, z) = \text{const}; \tag{8}$$

(ii) the convective and radiative heat exchange are specified on the surface contacting with the atmosphere, i.e.,

$$\begin{aligned}&-\left(k_x\frac{\partial T}{\partial x}l + k_y\frac{\partial T}{\partial y}m + k_z\frac{\partial T}{\partial z}n\right)\\ &= h(T - T_\infty) + \varphi\varepsilon c_0\left(T^4 - T_\infty^4\right),\end{aligned} \tag{9}$$

where $h$ is the convective heat exchange coefficient, $W/(m^2\ K)$; $T_\infty$ is the ambient temperature; φ is the angular coefficient of radiation; ε is the emissivity factor; $c_0 = 5.6687 \times 10^{-8}\ W/(m^2\ K^4)$ is the black body emissivity; and $l$, $m$, and $n$ are the areas of the contacting surface, $m^2$.

### *Statement of the Problem and Initial Data for Modeling*

We investigated the influence of the additive of lead (II) oxide into the KCl–$PbCl_2$ electrolyte, levels of the cathodic and anodic metals, and arrangement of the cathodic crucible on the spatial distribution of the dc current and temperature in a crucible-in-crucible type electrolyzer with liquid-metal electrodes, which was considered a typical facility for pyroelectrochemical processing of spent nuclear fuel.

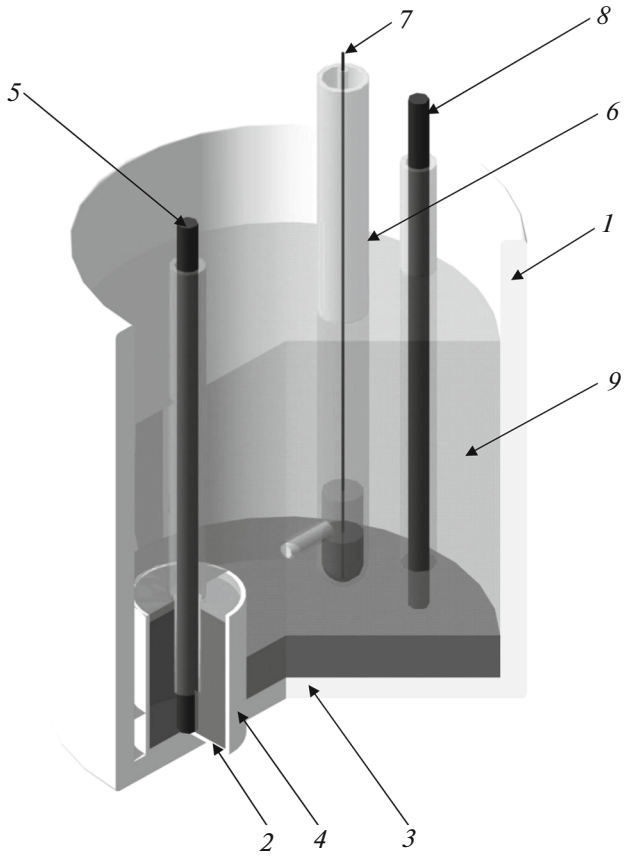


**Fig. 1.** Laboratory cell with liquid-metal lead electrodes. (*1*) Anodic fused alumina cup, (*2*) cathodic lead C1, (*3*) anodic lead C1, (*4*) cathodic fused alumina cup, (*5*) cathodic current led, (*6*) lead probe electrode, (*7*) molybdenum wire, (*8*) anodic current led, and (*9*) electrolyte.

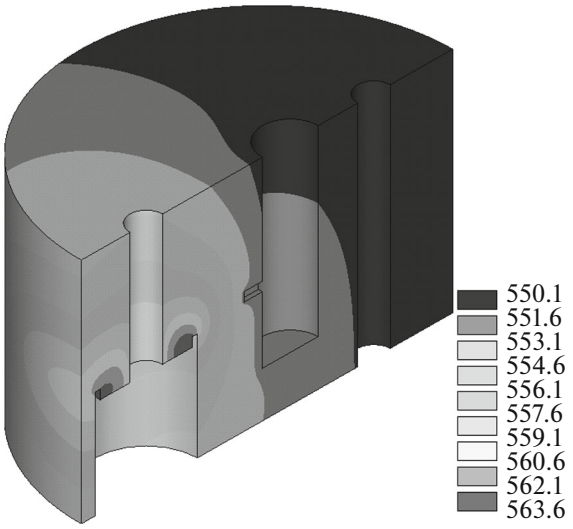


**Fig. 2.** Electrolyte temperature field (°C).

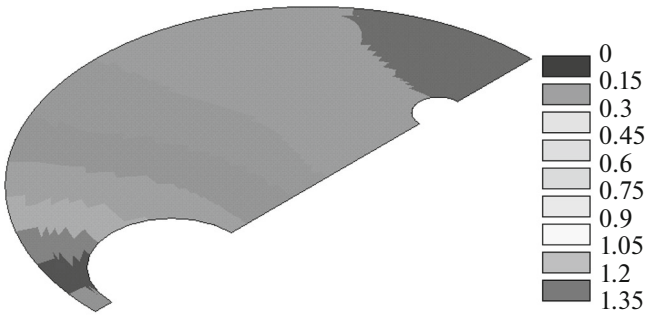


**Fig. 3.** Current density distribution (A/cm$^2$) along the metal–electrolyte surface.

The electrolyzer design is presented in Fig. 1. Physicochemical data for the electrolyte, electrodes, and construction materials necessary for calculations are described in [17–23].

### *Solution Method of Differential Equations*

Differential equations in partial derivatives of the electric and temperature fields were solved by the finite element method with the help of the ANSYS commercial software package.

## RESULTS OF MODELING

Abundant data on the distribution of the current density and temperature in the electrolyzer on the surface of liquid-metal electrodes and in the electrolyte volume are found in the course of mathematical modeling. Figures 2 and 3 show some of them in a graphical form. An equimolar mixture of lead and potassium chlorides (50 : 50 mol %) is used as the electrolyte. Electrodes are liquid-metal lead C1; the electrolyte level is 30 mm; and levels of cathodic and anodic metals are 30 and 10 mm, respectively.

The results of calculations showed that the electrolyte is overheated due to the evolution of the Joule heat by 13.6 K over the surface of the cathodic lead owing to the very high current density (Fig. 2). Recalculation of the electric field allowing for the results of calculations of the temperature field showed that the cell voltage decreased by 331 mV because of an increase in the electrolyte temperature and electrical conductivity.

### *Influence of the Electrolyte Composition*

When studying the influence of the electrolyte composition, we revealed the following peculiarities in the variation in the temperature and current density.

(i) When introducing the lead(II) oxide additive into the electrolyte, the region of an increased current density on the surface of the liquid-metal electrode narrows and the maximal current density (0.94 A/cm$^2$) is implemented at a distance of 0–2 cm from the cathodic crucible wall. It is revealed when calculating the tempera-

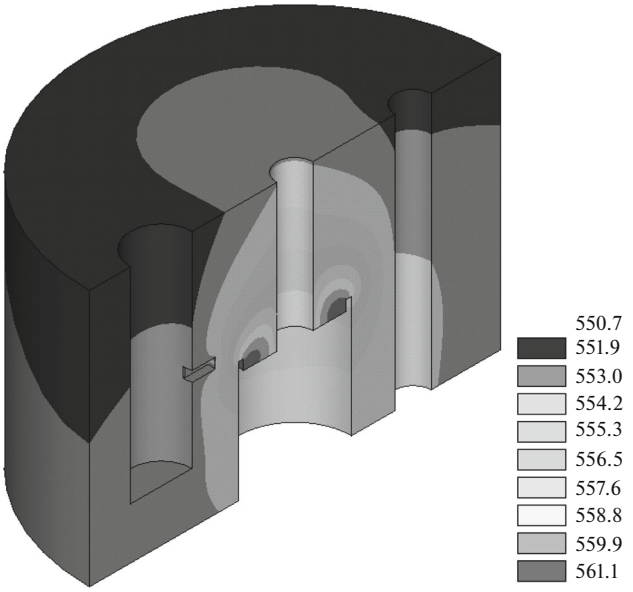


**Fig. 4.** Temperature field (°C) of the laboratory cell and electrolyte for the centered cathodic crucible arrangement.

ture field that the maximal temperature gradient is observed at a height of 0.5–1.0 cm over the cathodic crucible edge and being 45 K.

(ii) When introducing the additive of 0.5 wt % LiCl into the KCl–$PbCl_2$ electrolyte, the maximum of the anodic current density, which is implemented near the cathodic crucible wall, decreased from 0.9 to 0.75 A/$cm^2$, while the current lines are determined more uniformly. This circumstance had led to a decrease in the temperature gradient over the electrolyte height above the crucible edge. The maximal temperature was 833 K above the cathodic crucible edge.

(iii) The maximum in the anodic current density decreased from 0.9 to 0.65 A/$cm^2$ with an increase in the lithium chloride concentration to 10.0 wt % compared with the electrolyte without the additive, i.e., approximately by 35%. The temperature field was identical to the previous variant with the additive of 5 wt % LiCl.

### *Influence of the Levels of the Cathodic and Anodic Metals*

When studying the influence of the cathodic metal level, we considered three variants, notably, 10, 20, and 30 mm at a constant level of anodic metal of 10 mm.

Lowering the level of cathodic metal from 30 to 10 mm led to an increase in the distribution nonuniformity of the current density along the anode surface. In the construction under consideration, the maximal current density in the anodic part increased by 3.9–

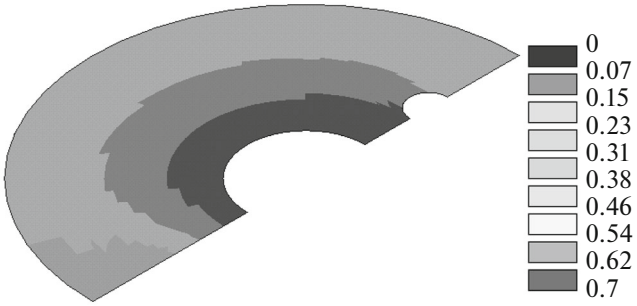


**Fig. 5.** Current density distribution (A/$cm^2$) in the electrolyte volume in the section at the metal–electrolyte interface for the centered cathodic crucible arrangement.

5.7%, while the maximal temperature in the electrolyte increased by 47.6 K. On the contrary, the maximal current density in the horizontal section above the cathodic cup decreased by 5.2%.

The investigation into the influence of the anodic metal level on the distribution of the electric and thermal fields is performed at a cathodic lead height of 30 mm. It is established that an increase in the anodic metal level from 10 to 30 mm led to a substantial increase in the distribution nonuniformity of the current density on the anode surface.

### *Influence of the Arrangement of the Cathodic Crucible*

In one of the variants, the cathodic crucible was established in the center of the anodic cup, as opposed to the previous experiments, where it was arranged near the anodic cup wall.

The results of calculations showed that such a geometric configuration of the electrolyzer made it possible to substantially decrease the nonuniformity in the current distribution. A decrease in maximal current densities on the anode surface by 14–16% and a decrease in the cell voltage by 10.0% were also observed.

Figures 4 and 5 show the results of calculations of the temperature field and current density distribution in the electrolyte volume for this sample.

## RESULTS AND DISCUSSION

The authors of [13, 24] described the experiments on the influence of temperature, electrolyte composition, and levels of cathodic and anodic metals on the current density distribution over the surface of the liquid-metal anode in the electrolyzer of the crucible-in-crucible type for lead refinement.

The calculated and experimental distribution curves of the current density over the surface of the liquid-metal anode for all cases under consideration are similar. The comparison of the calculated and experi-

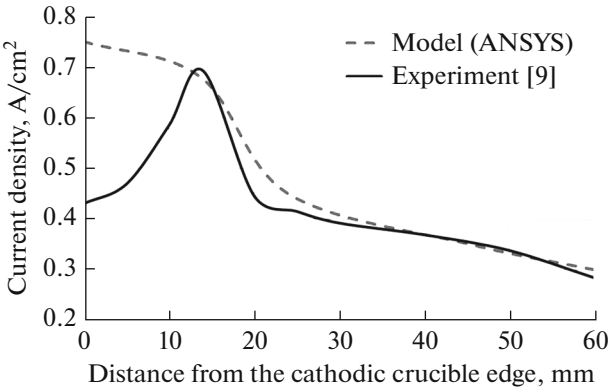


**Fig. 6.** Current density distribution along the surface of the liquid-metal anode for the variant with the additive of 5 wt % LiCl into the electrolyte.

mental data [13] for the variant with the additive of 5 wt % LiCl into the electrolyte are presented in Fig. 6 as an example. It is seen that the results of modeling and experimental data agree well between each other in a range from peak values of the anodic current density to its magnitude near the far wall of the anodic crucible. The model does not describe only the region near the cathodic crucible wall, where the so-called dead zone appears. This phenomenon can be explained from the viewpoint of physicochemical hydrodynamics [25].

Our results showed that, in order to attain more uniform current distribution and a lower consumption of electric power, the coaxial arrangement of crucibles with liquid-metal electrodes should be foreseen in the electrolyzer design.

In all considered variants, the results obtained in the course of mathematical modeling are in good agreement with the experimental data [13, 24]. This fact gives us grounds to believe that the developed model can be applied to other electrolytic systems with liquid-metal electrodes, in particular, to those recommended to regenerate spent nuclear fuel.

## CONCLUSIONS

We performed mathematical modeling of electrical and thermal fields in the electrolyzer with liquid-metal electrodes, according to the results of which the following is established:

(i) when introducing the lead (II) oxide additive, the region of an increased current density on the surface of the liquid-metal electrode narrows, while the maximal current density increases;

(ii) the maximum in the anodic current density drops compared with the electrolyte with no additive with an increase in the lithium chloride concentration;

(iii) an insignificant increase in the distribution nonuniformity of the current density along the anode surface and an increase in the maximal temperature in the electrolyte by 47.6 K are observed with lowering of the cathodic metal level;

(iv) an increase in the level of the anodic metal leads to a substantial increase in the distribution nonuniformity of the current density on the anode surface and to an increase in the anode surface with a current density lower than the geometric average.

The results of mathematical modeling agree well with the experimental data in the region from peak values of the current density to the edge point of the anodic surface in all cases. Their divergences with the experimental data do not exceed 3%. However, they do not describe the phenomenon of the appearance of the dead zone near the cathodic crucible edge, which can be explained from the viewpoint of the physicochemical hydrodynamics.

## ACKNOWLEDGMENTS

This study was supported by the Ministry of Education and Science of the Russian Federation, state contract no. 14.607.21.0084; the unique agreement identifier is RFMEF160714X0084.

## REFERENCES

1. Sakamura, Y., Shirai, O., Iwai, T., and Suzuki, Y., Distribution behavior of plutonium and americium in LiCl–KCl eutectic. Liquid cadmium systems, *J. Alloys Compd.*, 2001, vol. 321, pp. 76–83.
2. Hebditch, D., Hanson, B., Lewin, R., Beetham, S., Jenkins, J., and Sims, H., *Electrorefining of uranium and electro partitioning of U, Pu, Am, Nd and Ce*, in: Proc. of Global 2003, New Orleans, LA: pp. 1574–1581, 2003.
3. Satoh, T., Iwai, T., and Arai, Y., Electrolysis of burn up-simulated uranium nitride fuels in LiCl–KCl eutectic melts, *J. Nucl. Sci. Technol.*, 2009, vol. 46, pp. 557–563.
4. Song, K., Lee, H., Hur, J., Kim, J., Ahn, D., and Cho, Y., Status of pyroprocessing technology development in Korea, *Nucl. Eng. Technol.*, 2010, vol. 42, pp. 131–144.
5. Koyama, T., Sakamura, Y., Iizuka, M., Kato, T., Murakami, T., and Glatz, J.-P., Development of pyroprocessing fuel cycle technology for closing actinide cycle, *Proc. Chem.*, 2012, vol. 7, pp. 772–778.
6. Shirai, O., Uozumi, K., Iwai, T., and Arai, Y., Electrode reaction of the $U^{3+}$/U couple at liquid Cd and Bi electrodes in LiCl–KCl eutectic melts, *Anal. Sci.*, 2001, vol. 17, pp. 1959–1962.
7. Smolenski, V., Novoselova, A., Osipenko, A., and Kormilitsyn, M., and Luk'yanova Ya. Thermodynamics of separation of uranium from neodymium between the gallium–indium liquid alloy and the LiCl–KCl molten salt phases, *Electrochim. Acta*, 2014, vol. 133, pp. 354–358.
8. Smolenski, V., Novoselova, A., Osipenko, A., and Maershin, A., Thermodynamics and separation factor of uranium from lanthanum in liquid eutectic gallium-

indium alloy/molten salt system, *Electrochim. Acta*, 2014, vol. 145, pp. 81–85.

9. Omel'chuk, A.A., Thin-layered electrolysis in molten electrolytes, *Russ. J. Electrochem*, 2007, vol. 43, pp. 1007–1015.
10. Delimarski, Yu.K. and Zarubitski, O.G., *Electrolitcheskoe rafinirovanie tyazholykh metallov v ionnykh rasplavakh* (Electrolytic Refining of Heavy Metals in Ionic Melts), Moscow: Metallurgiya, 1975.
11. Delimarski, Yu.K., *Teoreticheskie osnovy electroliza ionnyh rasplavov* (Theoretical Foundations of Electrolysis of Ionic Melts), Moscow: Metallurgiya, 1986.
12. Omel'chuk, A.A., Electrorefining of heavy nonferrous metals in molten electrolytes, *Russ. J. Electrochem.*, 2010, vol. 46, pp. 680–690.
13. Efremov, A.N., Khalimullina, Yu.R., Pershin, P.S., Arkhipov, P.A., and Zaikov, Yu.P., Influence of the electrolyte composition on the current distribution in an electrolytic cell with liquid metal electrodes, Russ. Metallurgy (Metally), 2015, no. 2, pp. 115–120.
14. Ivanov, V.T., Scherbinin, S.A., and Galimov, A.A., *Matematicheskoe modelirovanie electroteplomassoperenosa v slozhnykh sistemakh* (Mathematical Modeling of Electrical and Heat-and-Mass Transfer in Complex Systems), Ufa: Bashkir. Nauch. Tsentr., Ural Otr. Ross. Akad. Nauk SSSR, 1991.
15. Bessonov, L.A., *Teoreticheskie osnovy electrotehniki. Electromagnitnoe pole* (Fundamentals of Electrical Engineering. Electromagnetic Field), Moscow: Vysshaya Shkola, 1978.
16. Segerlind, L., Primenenie metoda konechnyh elementov (Application of the Finite Element Method), Moscow: Mir, 1979.
17. Balkevich, V.L., *Tehnicheskaya keramika,* (Technical Ceramics: Textbook for Technical Higher Schools), Moscow: Stroiizdat, 1984.
18. ASM Metals Handbook. Vol. 1: *Properties and Selection: Irons, Steels, and High-Performance Alloys*, OH: ASM, 1990, 10th ed.
19. Desai, P.D., Chu, T.K., James, H.M., and Ho, C.Y., Electrical resistivity of selected elements, *J. Phys. Chem. Ref. Data*, 1984, vol. 13, no. 4, pp. 1069–1096.
20. Shinno, H., Kitajima, M., and Okada, M., Thermal stress analysis of high heat flux materials, J. Nucl. Mater., 1988, vol. 155–157, pp. 290–294.
21. Giordanengo, B., Benazzi, N., Vinckel, J., Gasser, J.G., and Roubi, L., Thermal conductivity of liquid metals and metallic alloys, J. Non-Cryst. Solids, 2000, vol. 250–252, pp. 377–383.
22. Gale, W.F. and Totemeier, T.C., *Smithells Metals Reference Book*, Amsterdam: Elsevier, 1988.
23. Iida, T. and Guthrie, R.I.L., *The Physical Properties of Liquid Metals*, Oxford: Clarendon, 1988.
24. Efremov, A.N., Arkhipov, P.A., and Zaikov, Yu.P., Simulation of the electric field in an electrolytic cell with a liquid metal anode, Russ. Metallurgy (Metally), 2013, no. 2, pp. 96–99.
25. Levich, V.G., *Fiziko-khimicheskaya gidrodinamika* (Physicochemical Hydrodynamics), Moscow: Gos. Izd. Fiz.-Mat. Lit., 1959.

*Translated by N. Korovin*